Journal of Physics: Conference Series **2796** (2024) 012007 doi:10.1088/1742-6596/2796/1/012007

Stellar models with like-Wyman IIa complexity factor

J. Andrade[1], D. Andrade[2].

[1]Escuela de Física y Matemática, Facultad de Ciencias, Escuela Superior Politécnica de Chimborazo, Riobamba, Ecuador.
[2]School of Physical Sciences and Nanotechnology, Yachay Tech University, 100119 Urcuquí, Ecuador.

E-mail: julio.andrade@espoch.edu.ec

January 2024

Abstract. The goal of this work is to build a new family of stellar interior solutions in the anisotropic regime of pressure using the framework of gravitational decoupling via minimal geometric deformation. For such purpose, we use a generalization of the complexity factor of the well-known Wyman IIa ($n = 1$) interior solution in order to close the Einstein's Field Equations, as well we use the Wyman IIa, Tolman IV, and Heintzmann IIa and Durgapal IV models as seeds solutions. These models fulfill the fundamental physical acceptability conditions for the compactness factor of the system 4U 1820-30. Stability against convection and against collapse are also studied.

Keywords: Interior solutions, gravitational decoupling, complexity factor

1. Introduction

In the context of General Relativity, stellar systems were thought to be described by isotropic stellar solutions for a very long time. Thus many models have been developed since Karl Schwarzschild in 1916 found the first exact solution of Einstein's Field Equations (EFE) [1]. Examples of such models are found in several works [2–32]. However, the assumption of modeling a stellar system using isotropic models results in mathematical models that are incapable of describing more realistic and complex systems since it is well known that a wide range of physical processes of the sort that are anticipated in compact objects may induce disturbances of the isotropy and fluctuations of the local anisotropy in pressure [33]. Indeed, there are numerous physical processes that could occur in high energy density stellar systems, resulting in local anisotropy in the system [34]. This local anisotropy can be caused by a wide variety of physical phenomena that can be found in stellar compact objects. For instance, this type of phenomenon includes a recombination of fluids, the existence of super-fluids, the presence of a solid core, phase transitions, and the presence of magnetic fields,

among others [35–52]. In fact, if the system has a regime of isotropic pressure, the resulting final stage of stellar evolution should have anisotropic pressure [53]. Even so, it is worth mentioning that the presence of anisotropy is frequently observed as a repulsive force that counterbalances the gravitational force and contributes to the system's stability [54, 55]. As a result, the goal of obtaining new anisotropic stellar solutions is highly valued.

For spherically symmetric space-times, whose metric can be written in canonic coordinates, which has two radial functions ν and λ [19] (see Eq. (3)), the framework of solving the EFE results in a robust problem where there are three independent differential equations containing five unknown functions: two geometric functions ($\nu(r)$ and $\lambda(r)$), and three physical functions energy density ρ, radial pressure p_r and tangential pressure p_t (referred to as the solution's matter sector). As a result, in order to close the EFE, two additional conditions must be imposed, which can be metric function relations or state equations that relate physical quantities. Particularly, in this manuscript, we use a recently successful framework to solve the EFE well-known as Gravitational Decoupling (GD) through Minimal Geometric Deformation (MGD) [56–60](for the extended version of MGD see [61]). In this approach, a known interior solution is used (a perfect fluid solution is typically used, but an anisotropic solution can also be used) as seed solution in order to obtain a new interior solution, which is commonly in the anisotropic regimen of pressure. However, to perform this, it is still necessary to add an extra condition to close the system of equations. Use of equations of state, conditions on density and pressure, metric conditions are a few criteria that have been mentioned in the literature [62–87].

In particular, we use the known complexity factor for self-gravitating spheres as extra conditions to close the EFE that arises from the use of GD through MGD. In such a sense, we obtain a new family of anisotropic solutions that fulfills the acceptance conditions for a realistic stellar compact object. This complexity factor surges from Herrera's definition [88, 89], which is related to the notion of the interior structure of the self-gravitating spherical system; specifically, it is based on the idea that the simplest compact stellar object is the one that is a perfect fluid (incompressible and isotropic in its pressure components), and therefore more complex systems are those that present inhomogeneities in energy density and isotropic pressure deviations. In particular, the complexity criteria is a cutting-edge instrument that enables us to create new anisotropic solutions, as a result of which new solutions have recently been found given the use of this factor in [90–103]. But also, this definition is so adequate that it has allowed to carry out, its implementation on the study of black holes in the framework of the Newman–Penrose formalism [104], construct traversable wormholes geometries [105, 106], an study of the departure from spheroidicity of self-gravitating spheres [107], its extension for the time dependent case [108], the study of the dynamics of the gravitational collapse of a compact object [109], for study of axially symmetric systems [110, 111], for the study of cylindrical fluid systems [112–114], even it has been used in the study of symmetric hyperbolical fluids [115–128], among others.

This paper is organized as follows: In Sect. 2 we briefly review the EFE and the main aspects of GD via MGD. In Sect. 3 we introduce the matching conditions. In Sect. 4 we present the physical acceptability conditions, which will be used to test the new interior solutions. In Sect. 5 we provided a brief revision about the complexity of compact sources. In Sect. 6 we found a generalization of the complexity factor for the Wyman IIa interior solution. In Sects. 7-10, the new models are found by using the GD through MGD with the Wyman IIa, Tolman IV, Heintzmann IIa and Durpagal IV solutions as isotropic seeds and the generalization of Wyman IIa ($n = 1$) as an extra condition. Finally, in Sect. 11 we discuss the physical acceptance and stability of the new models.

2. Einstein's field equations and gravitational decoupling

In this section, we will briefly discuss the main aspects of gravitational decoupling (GD) via minimal geometric deformation (MGD). The GD approach allows us to solve the Einstein field equations (EFE)

$$G_{\mu\nu} \equiv R_{\mu\nu} - \frac{1}{2} g_{\mu\nu} R = \kappa T_{\mu\nu}, \tag{1}$$

where

$$T_{\mu\nu} = T^{(s)}_{\mu\nu} + \alpha \theta_{\mu\nu} \ , \tag{2}$$

with $\kappa = \dfrac{8\pi G}{c^4}$‡, $T^{(s)}_{\mu\nu} = diag[\rho^{(s)}, p_r^{(s)}, p_t^{(s)}, p_t^{(s)}]$ is the matter sector of a known solution (known as the matter sector of the seed solution), $\theta_{\mu\nu} = diag[\theta^0_0, \theta^1_1, \theta^2_2, \theta^3_3]$ is the matter sector of an unknown extra source and α is a dimensionless factor that measures the intensity coupling between both sources in EFE.

The corresponding space-time solution of Eq. (1) is related to the interior of a static self-gravitating system in spherically symmetric space-time, represented by the line element parametrized as

$$ds^2 = e^{\nu} dt^2 - e^{\lambda} dr^2 - r^2 (d\theta^2 + \sin^2\theta d\phi^2), \tag{3}$$

where ν and λ are functions that depend only on the radial coordinate r. In what follows, using the Eq. (3) in Eq. (1) and considering the Eq. (2), we arrive at

$$\kappa\rho \ = \frac{1}{r^2} + e^{-\lambda}\left(\frac{\lambda'}{r} - \frac{1}{r^2}\right), \tag{4}$$

$$\kappa p_r = \ -\frac{1}{r^2} + e^{-\lambda}\left(\frac{\nu'}{r} + \frac{1}{r^2}\right), \tag{5}$$

$$\kappa p_t = \frac{e^{-\lambda}}{4}\left(2\nu'' + \nu'^2 - \lambda'\nu' + 2\frac{\nu' - \lambda'}{r}\right), \tag{6}$$

‡ In this work we shall use $G = c = 1$.

where a new matter sector is defined as

$$\rho = \rho^{(s)} + \theta_0^0 \,, \tag{7}$$
$$p_r = p_r^{(s)} - \theta_1^1 \,, \tag{8}$$
$$p_t = p_t^{(s)} - \theta_2^2 \,. \tag{9}$$

The way we have introduced the energy-momentum tensor in the expression (2) brings to light a simple separation of the constituents of the matter sector, but due to the non-linearity of the EFE, it seems a priori that it is not possible to separate into two groups of equations for each constituent. However, it is feasible in the context of the GD.

The core concept of GD is to introduce a geometric deformation that affects the space-time of the seed solution (solution of (1) when $T_{\mu\nu} = T_{\mu\nu}^{(s)}$) given by

$$ds^2 = e^{\xi} dt^2 - e^{\mu} - r^2(d\theta^2 + \sin^2\theta d\phi^2), \tag{10}$$

in order to codify the influence of the unknown source $\theta_{\mu\nu}$ over $T_{\mu\nu}$, in the following way

$$\nu \longrightarrow \xi + \alpha g, \tag{11}$$
$$e^{-\lambda} \longrightarrow e^{-\mu} + \alpha f, \tag{12}$$

where $\{\xi, \mu\}$ are functions only of radial coordinate r, $\{f, g\}$ are the so-called decoupling functions and α is the same parameter in Eq. (2). In general, one could consider the two deformations in both metrics (radial and temporal), however, in this work we shall use the MGD approach, in which the decoupling functions $g = 0$ and $f \neq 0$. Now applying the MGD technique, we can straightforwardly split the system of equations (4)-(6) into two sets; the first one is obtained by doing $\alpha = 0$, and it reads as

$$\kappa\rho^{(s)} = \frac{1}{r^2} - e^{-\mu}\left(\frac{1}{r^2} - \frac{\mu'}{r}\right), \tag{13}$$
$$\kappa p^{(s)} = -\frac{1}{r^2} + e^{-\mu}\left(\frac{1}{r^2} + \frac{\xi'}{r}\right), \tag{14}$$
$$\kappa p^{(s)} = \frac{e^{-\mu}}{4}\left(2\xi'' + \xi'^2 - \mu'\xi' + 2\frac{\xi' - \mu'}{r}\right). \tag{15}$$

The second set of equations is obtained by turning on the parameter α, i.e., $\alpha \neq 0$, so that contains the effects of the source $\theta_{\mu\nu}$ and reads

$$\kappa\theta_0^0 = -\frac{f}{r^2} - \frac{f'}{r}, \tag{16}$$
$$\kappa\theta_1^1 = -f\left(\frac{1}{r^2} + \frac{\nu'}{r}\right), \tag{17}$$
$$\kappa\theta_2^2 = -\frac{f}{4}\left(2\nu'' + \nu'^2 + \frac{2\nu'}{r}\right) - \frac{f'}{4}\left(\nu' + \frac{2}{r}\right). \tag{18}$$

Furthermore, the contracted Bianchi identities ensure that the Einstein tensor is divergence-free. Then, by the Eq. (1), we can derive the covariant conservation of the energy-momentum tensor as follows:

$$\nabla_\mu T^{\mu\nu} = 0. \tag{19}$$

Furthermore, $T^{(s)}_{\mu\nu}$ satisfies the following conservation equation

$$\nabla_\mu T^{(s)}_{\mu\nu} = p'^{(s)} + \frac{\nu'}{2}(\rho^{(s)} + p^{(s)}) = 0, \tag{20}$$

since $T^{(s)}_{\mu\nu}$ corresponds to a known "seed" source that satisfies its respective EFE. Note that Eq. (20) is a linear combination of Eqs. (13)-(15). Thus, automatically, the source $\theta_{\mu\nu}$ fulfills the following expression

$$\nabla_\mu \theta^{\mu\nu} = \left(\theta^1_1\right)' + \frac{\nu'}{2}\left(\theta^0_0 - \theta^1_1\right) + \frac{2}{r}\left(\theta^2_2 - \theta^1_1\right) = 0. \tag{21}$$

It is worth noticing that Eq. (21) can also be obtained as a linear combination of Eqs. (16)-(18). Furthermore, note that Eqs. (20) and (21) imply that the interaction between the source $T_{\mu\nu}$ and the source $\theta_{\mu\nu}$ is purely gravitational, i.e., there is no exchange of energy-momentum.

3. Matching conditions

At the boundary of the stellar compact object ($r = R$), the metric components e^ν and $e^{-\lambda}$ should match continuously with the Schwarzschild exterior solution, namely

$$e^\nu|_{r=R} = e^{-\lambda}|_{r=R} = 1 - \frac{2M}{R}, \tag{22}$$

where M and R are the total mass and radius of star, respectively.

As also is necessary that

$$p_r(r = R) = 0 \tag{23}$$

since the exterior of star in this case is considered empty.

4. Physical acceptability conditions

The fundamental physical requirements necessary to any interior solution can describe a realistic stellar compact object are (see Ref [129] for a detailed discussion of these conditions):

C1. In the interior of a stellar compact object, the metrics e^ν and e^λ should be finite and regular; additionally, $e^{-\nu(0)} = constant$ and $e^{-\lambda(0)} = 1$.

C2. The matter sector given by the density energy ρ, radial pressure p_r and transversal pressure p_t should be positive and regular inside the compact object. They should be decreasing functions of the radial coordinate r, with their maximum values at the center. Furthermore, the radial pressure should vanish at the boundary, and $p_r|_{r=0} = p_t|_{r=0}$.

C3. The Dominant Energy Condition (DEC) $\rho - p_r \geq 0$ and $\rho - p_t \geq 0$ should be fullfiled inside the stellar compact object.

C4. The surface redshift $z(r) = g_{tt}^{-1/2}(r) - 1$ should decrease outward and its value at the surface is less than the universal bound for interior solutions satisfying the DEC, namely $z_{bound} = 5.211$ [130].

C5. The stability of the stellar object requires that the fluid speed of sound should be less than the speed of light, which leads $0 \leq v_r = \sqrt{\frac{dp_r}{d\rho}} \leq 1$ and $0 \leq v_t = \sqrt{\frac{dp_t}{d\rho}} \leq 1$ within a stellar compact object.

5. Complexity of compact sources

The concept of complexity is highly dependent on the subject of study, particularly, in this work, we shall use a definition of complexity for static and spherically symmetric self-gravitational systems, which was recently proposed by L. Herrera [88, 89] in the context of general relativity. This definition is based on the idea that the simplest system is the one with perfect fluid distribution and that more complex systems are those that vary from this fundamental system, especially those that deviate from the regular pattern of constant energy density and pressure isotropy.

Specifically, such a definition surges from the existence of a structure scalar that is connected to the orthogonal splitting of the Riemann tensor [131, 132] in static and spherically symmetric space-times (for the first time, such a scalar and others were thoroughly examined in [133]). This scalar captures the concept of complexity since it measures the relationship between the inhomogeneity in the energy density and the pressure anisotropy of a static and spherically symmetric self-gravitational system. This scalar is given by

$$Y_{TF} = \kappa\Pi - \frac{\kappa}{2r^3}\int_0^r \tilde{r}^3\rho' d\tilde{r}, \tag{24}$$

with $\Pi \equiv p_r - p_t$.

Additionally, it can be demonstrated that (24) permits one to express the Tolman mass as

$$m_T = (m_T)_\Sigma \left(\frac{r}{r_\Sigma}\right)^3 + r^3 \int_r^{r_\Sigma} \frac{e^{(\nu+\lambda)/2}}{\tilde{r}} Y_{TF} d\tilde{r}, \tag{25}$$

which, includes all the alterations caused by the energy density inhomogeneity and the anisotropy of the pressure on the active gravitational mass, namely, the Tolman mass, which is a combination of its value for a zero-complexity system and two other terms related to energy density inhomogeneity and pressure anisotropy, respectively. It can be viewed as a convincing justification to define the complexity factor by means of this scalar. Thus, this scalar represents an appropriate parameter that characterizes the complexity of self-gravitating static spheres since, firstly, it is based on a structure scalar (which is critical because it ensures that this characteristic is founded on a quantity that is invariant for any observer) that contains all physical parameters of the matter sector

of the interior of the self-gravitating sphere, and very particularly, it depends on the inhomogeneity in the energy density and the anisotropy in the pressure, which is in perfect relation that the most simplest system is the perfect fluid sphere and the more complex are those who move away from that system.

Now, it is worth noticing that if one uses the EFE (4)-(6) in (24) arrives at

$$Y_{TF} = \frac{e^{-\lambda}}{4r}\left(\nu'(2 + r\lambda' - r\nu') - 2r\nu''\right), \tag{26}$$

which represents an alternative way to calculate Y_{TF} through the knowledge of the space-time inside of a compact source.

Particularly, Eq. (24) has been used as a state equation in order to construct new interior solutions for self-gravitating spheres. For example, it is significant to note that the vanishing complexity criterion, often known as the $Y_{TF} = 0$ condition, is met not only in the most straightforward instances of isotropic and homogeneous systems, but also in the situations where

$$\Pi = \frac{1}{2r^3}\int_0^r \tilde{r}^3\rho' d\tilde{r}, \tag{27}$$

namely, in the scenarios where the pressure anisotropy and energy inhomogeneity cancel each other.

The system of EFE can be closed using Eq. (27) as a complementing condition because it reflects a non-local equation of state (an interesting formalism to construct solutions with such a characteristic is developed recently in [101]). However, one can explore different values of the complexity factor distinct from zero in order to find new solutions, so in this work, a specific value for this scalar is proposed in the next section.

6. The generalized Wyman IIa complexity factor

In this current work, we use as an extra condition a specific value of the complexity factor in order to close the EFE resulting from GD through MGD. Thus, in order to use its complexity factor as a supplementary condition, we use the Wyman IIa (with $n = 1$) [20, 134] solution given by the following metrics

$$e^{\xi} = \left(A_0 - B_0 r^2\right)^2 \tag{28}$$

$$e^{-\mu} = 1 + \frac{C_0 r^2}{\left(A_0 - 3B_0 r^2\right)^{2/3}}, \tag{29}$$

where A_0 is a dimensionless constant, B_0 and C_0 are constants with units of $length^{-2}$. So in such a way, we replace Eqs.(28) and (29) in (26) to obtain

$$Y_{TF} = \frac{2B_0 C_0 r^2}{\left(A_0 - 3B_0 r^2\right)^{5/3}}, \tag{30}$$

which can be generalized as

$$Y_{TF} = \frac{a_1 r^2}{\left(a_2 + a_3 r^2\right)^{5/3}}, \tag{31}$$

where a_1 is an arbitrary constant with units of $length^{-4}$, a_2 is an arbitrary dimensionless constant, and a_3 must be a constant with units of $length^{-2}$.

Using Eq. (12) in (26) yields the following differential equation:

$$\frac{\alpha\xi'}{4}f' + \frac{\alpha}{2}\left(\xi'' - \frac{\xi'}{r} + \frac{\xi'^2}{2}\right)f + \frac{e^{-\mu}}{2}\left(\xi'' - \frac{\xi'}{r} + \frac{\xi'^2}{2} - \frac{\mu'\xi'}{2}\right) + Y_{TF} = 0, \tag{32}$$

which permits us to obtain the decoupling function f given the pair $\{\xi, \mu\}$ (the seed solution) and a specific value of Y_{TF}.

7. Model 1: like-Wyman IIa solution

In this part, we shall obtain a new interior solution with the Wyman IIa ($n = 1$) complexity factor. In such a sense, we use as a seed solution the Wyman IIa (with $n = 1$) given by (28) and (29) in (32), obtaining

$$f(r) = c_1 - \frac{\frac{4C_0 r^2}{(A_0 - 3B_0 r^2)^{2/3}} + \frac{3a_1\left(a_3A_0 + 3a_2B_0 + 2a_3B_0r^2\right)}{a_3^2 B_0 (a_2 + a_3 r^2)^{2/3}}}{4\alpha} \tag{33}$$

where c_1 is an integration constant. Thus, taking this f in Eq.(12), we obtain the new radial metric given by

$$e^{-\lambda} = 1 + \alpha c_1 - \frac{3a_1\left(a_3A_0 + 3a_2B_0 + 2a_3B_0r^2\right)}{4a_3^2 B_0\left(a_2 + a_3r^2\right)^{2/3}}. \tag{34}$$

However, such a value of $e^{-\lambda}$ leads us to have a material sector with divergence problems. Therefore, in order to solve this problem, it can be prove that the constant c_1 must satisfy

$$c_1 = \frac{3a_1(a_3A_0 + 3a_2B_0)}{4\alpha a_2^{2/3} a_3^2 B_0}. \tag{35}$$

Thus, $e^{-\lambda}$ is redefined as

$$e^{-\lambda} = 1 + \frac{3a_1\left(\frac{a_3A_0}{a_2^{2/3}B_0} - \frac{a_3A_0 + 3a_2B_0 + 2a_3B_0r^2}{B_0(a_2 + a_3r^2)^{2/3}} + 3\sqrt[3]{a_2}\right)}{4a_3^2}. \tag{36}$$

Now, from the system (4)-(6) we arrive at

$$\rho = \frac{a_1}{4a_2^{2/3}a_3^2B_0\kappa r^2\chi(r)^{5/3}}\left[a_2^{2/3}\varphi_1(r) - 3\chi(r)^{5/3}(a_3A_0 + 3a_2B_0)\right] \tag{37}$$

$$p_r = -\frac{1}{\kappa r^2}\left[1 - \left(5 - \frac{4A_0}{A_0 - B_0r^2}\right) \times \left(1 + \frac{3a_1\left(\frac{a_3A_0}{a_2^{2/3}B_0} - \frac{\varphi_2(r)}{B_0\chi(r)^{2/3}} + 3\sqrt[3]{a_2}\right)}{4a_3^2}\right)\right] \tag{38}$$

$$p_t = -\frac{1}{2\kappa}\left[\frac{8B_0}{A_0 - B_0r^2} + \frac{3a_1\varphi_3(r)}{a_3^2\left(B_0r^2 - A_0\right)\chi(r)^{5/3}} + a_1A_0\left(\frac{6}{a_2^{2/3}\left(a_3A_0 - a_3B_0r^2\right)} - \frac{1}{B_0\chi(r)^{5/3}}\right)\right], \tag{39}$$

where the functions $\chi(r)$, $\varphi_1(r)$, $\varphi_2(r)$ and $\varphi_3(r)$ are auxiliary functions (see the Appendix, Sect. 13).

Finally, the continuity of the first and second fundamental forms leads to

$$a_1 = \frac{16a_2^{2/3}a_3^2B_0^2R^2\chi(R)^{2/3}}{3\left(A_0 - 5B_0R^2\right)}\left[\left(a_3A_0 + 3a_2B_0\right)\chi(R)^{2/3} - 3a_2^{5/3}B_0 - a_2^{2/3}a_3\left(A_0 + 2B_0R^2\right)\right], \tag{40}$$

$$A_0 = \frac{B_0R^2(5M - 2R)}{M}, \tag{41}$$

$$B_0^2 = \frac{M^2}{4R^5(R - 2M)}, \tag{42}$$

with $\chi(R) = \chi|_{r=R}$.

It is worth noting that $R > 2M$ is derived from Eq. (41), which is consistent with the requirement that any stable configuration should be greater than its Schwarzschild radius.

8. Model 2: like-Tolman IV solution

In this case, we use the Tolman IV solution [19] as a seed solution, which is given by

$$e^{\xi} = B^2\left(\frac{r^2}{A^2} + 1\right), \tag{43}$$

$$e^{-\mu} = \frac{\left(A^2 + r^2\right)\left(C^2 - r^2\right)}{C^2\left(A^2 + 2r^2\right)}, \tag{44}$$

where A, B and C are constants. So, realizing the same procedure as in the last section, but using the Tolman IV solution, we obtain

$$f = \frac{A^2 + r^2}{2\alpha C^2}\left[\frac{2C^2}{A^2} - \frac{2(C - r)(C + r)}{A^2 + 2r^2} + \frac{3a_1C^2\left(\frac{1}{\chi(r)^{2/3}} - \frac{1}{a_2^{2/3}}\right)}{a_3}\right], \tag{45}$$

with which in (4) we arrives at

$$e^{-\lambda} = \frac{A^2+r^2}{2A^2 a_2^{2/3} a_3 \chi(r)^{2/3}}\left[2a_2^{2/3} a_3 \chi(r)^{2/3} + 3A^2 a_1\left(a_2^{2/3} - \chi(r)^{2/3}\right)\right]. \quad (46)$$

Now, using EFE (4)-(6), one obtains the new matter sector

$$\rho = \frac{1}{2\kappa}\Bigg[-\frac{6}{A^2} + \frac{a_1}{a_3}\left(\frac{9}{a_2^{2/3}} - \frac{9a_2+5a_3r^2}{\chi(r)^{5/3}}\right) + \frac{a_1 A}{a_3 r^2}\left(\frac{3}{a_2^{2/3}} + \frac{a_3 r^2 - 3a_2}{\chi(r)^{5/3}}\right)\Bigg] \quad (47)$$

$$p_r = \frac{3}{2\kappa}\left[\frac{2}{A^2} + \frac{3a_1}{a_3}\left(\frac{1}{\chi(r)^{2/3}} - \frac{1}{a_2^{2/3}}\right) + \frac{a_1 A^2}{a_3 r^2}\left(\frac{1}{\chi(r)^{2/3}} - \frac{1}{a_2^{2/3}}\right)\right] \quad (48)$$

$$p_t = \frac{1}{\kappa}\left[\frac{6}{A^2} - \frac{9a_1}{a_2^{2/3} a_3} + \frac{a_1\left(-2a_3A^2 + 9a_2 + 5a_3r^2\right)}{a_3\chi(r)^{5/3}}\right] \quad (49)$$

Now, applying the matching conditions, we obtain the following

$$a_1 = \frac{2a_2^{2/3} a_3 R^2 \chi(R)^{2/3}}{A^2\left(A^2+3R^2\right)\left(\chi(R)^{2/3} - a_2^{2/3}\right)}, \quad (50)$$

$$A^2 = \frac{R^2(R-3M)}{M}, \quad (51)$$

$$B^2 = 1 - \frac{3M}{R}. \quad (52)$$

9. Model 3: like-Heintzmann IIa solution

In this case, we consider the Heintzmann IIa solution [20, 135] as a seed, which is given by

$$e^{\xi} = A^2\left(Br^2+1\right)^3, \quad (53)$$

$$e^{-\mu} = 1 - \frac{3Br^2\left(1 + \frac{C}{\sqrt{4Br^2+1}}\right)}{2\left(Br^2+1\right)}, \quad (54)$$

where A, B and C are constants. Then, using the same procedure as in the previous sections, we found

$$f = \frac{1}{12\alpha B\left(Br^2+1\right)}\Bigg[6B^2r^2 + \frac{18B^2Cr^2}{\sqrt{4Br^2+1}} - \frac{3a_1\left(9a_2^2B^2 - 12a_2a_3B + 2a_3^2\right)}{a_2^{2/3}a_3^3} + \frac{3a_1\left(9a_2^2B^2 + 6a_2a_3B\left(Br^2-2\right)\right)}{a_3^3\chi(r)^{2/3}} - \frac{3a_1\left(a_3^2\left(Br^2\left(Br^2+8\right)-2\right)\right)}{a_3^3\chi(r)^{2/3}}\Bigg]. \quad (55)$$

In such a sense, the new radial metric is

$$e^{-\lambda} = \frac{1}{4\left(Br^2+1\right)}\Bigg[\frac{a_1\left(-9a_2^2B^2+12a_2a_3B-2a_3^2\right)}{a_2^{2/3}a_3^3B} + \frac{a_1\left(9a_2^2B^2+6a_2a_3B\left(Br^2-2\right)\right)}{a_3^3B\chi(r)^{2/3}} - \frac{a_1a_3^2\left(Br^2\left(Br^2+8\right)-2\right)}{a_3^3B\chi(r)^{2/3}}+4\Bigg]. \tag{56}$$

Now, using EFE (4)-(6), we arrive at

$$\rho = \frac{1}{12Br^2\left(Br^2+1\right)^2\kappa}\left[12B^2r^2\left(Br^2+3\right)+\frac{a_1\varphi_4(r)}{a_2^{2/3}a_3^3\chi(r)^{5/3}}\right], \tag{57}$$

$$p_r = -\frac{1}{\kappa r^2}\Bigg[1-\frac{7Br^2+1}{4\left(Br^2+1\right)^2}\Bigg(4+\frac{a_1\varphi_5(r)}{a_3^3B\chi(r)^{2/3}} + \frac{a_1\left(-9a_2^2B^2+12a_2a_3B-2a_3^2\right)}{a_2^{2/3}a_3^3B}\Bigg)\Bigg], \tag{58}$$

$$p_t = \frac{1}{12B\kappa\left(Br^2+1\right)^2}\left[\frac{a_1\varphi_6(r)}{a_2^{2/3}a_3^3\chi(r)^{5/3}}+60B^2\right], \tag{59}$$

where $\varphi_4(r)$, $\varphi_5(r)$ and $\varphi_6(r)$ are auxiliary functions defined in Sect. 13. Now from matching conditions we have

$$a_1 = \frac{4a_2^{2/3}a_3^3B^2R^2\left(BR^2-5\right)\chi(R)^{2/3}}{7BR^2+1}\Bigg[9a_2^{8/3}B^2 - a_2^{2/3}a_3^2\left(BR^2\left(BR^2+8\right)-2\right)+6a_2^{5/3}a_3B\left(BR^2-2\right) - \left(9a_2^2B^2+2a_3^2-12a_2a_3B\right)\chi(R)^{2/3}\Bigg]^{-1}, \tag{60}$$

$$B = \frac{M}{R^2(3R-7M)}, \tag{61}$$

$$A^2 = \frac{(3R-7M)^3}{27R(R-2M)^2}. \tag{62}$$

Eqs. (61) and (62) show that $M/R < 3/7 < 4/9$ corresponds to less compact solutions than the Buchdahl's limit allows for isotropic solutions.

10. Model 4: like-Durgapal IV solution

In this last case, we consider the Durgapal IV solution [20, 136] as a seed solution

$$e^{\xi} = A\left(Cr^2+1\right)^4, \tag{63}$$

$$e^{-\mu} = \frac{BCr^2}{\left(Cr^2+1\right)^2\left(5Cr^2+1\right)^{2/5}}+\frac{7-10Cr^2-C^2r^4}{7\left(Cr^2+1\right)^2}, \tag{64}$$

where A, B and C are constants. After realizing the same procedure applied in the last sections, we found the decoupling function

$$f = \frac{1}{112\alpha C\left(Cr^2+1\right)^2}\Bigg[160C^2r^2 + 16C^3r^4 - \frac{112BC^2r^2}{\left(5Cr^2+1\right)^{2/5}} + \frac{3a_1\varphi_7(r)}{a_3^4\chi(r)^{2/3}} + \frac{3a_1}{a_2^{2/3}a_3^4}\left(81a_2^3C^3 - 189a_2^2a_3C^2 + 126a_2a_3^2C - 14a_3^3\right)\Bigg], \tag{65}$$

where $\varphi_7(r)$ is an auxiliary function defined in Sect. 13. Thus, the resulting radial metric is

$$e^{-\lambda} = \frac{1}{112\left(Cr^2+1\right)^2}\Bigg[112 + \frac{3a_1\varphi_7(r)}{a_3^4C\chi(r)^{2/3}} + \frac{3a_1}{a_2^{2/3}a_3^4C}\left(81a_2^3C^3 - 189a_2^2a_3C^2 + 126a_2a_3^2C - 14a_3^3\right)\Bigg]. \tag{66}$$

Then, from EFE (4)-(6) we obtain

$$\rho = \frac{1}{112C\kappa\left(Cr^2+1\right)^3}\Bigg[112C^2\left(Cr^2\left(Cr^2+3\right)+6\right) + \frac{a_1\varphi_8(r)}{a_2^{2/3}a_3^4r^2\chi(r)^{5/3}}\Bigg], \tag{67}$$

$$p_r = -\frac{1}{\kappa r^2}\Bigg[1 - \frac{9Cr^2+1}{112\left(Cr^2+1\right)^3}\Bigg(112 + \frac{3a_1\varphi_9(r)}{a_3^4C\chi(r)^{2/3}} + \frac{3a_1}{a_2^{2/3}a_3^4C}\left(81a_2^3C^3 - 189a_2^2a_3C^2 + 126a_2a_3^2C - 14a_3^3\right)\Bigg)\Bigg], \tag{68}$$

$$p_t = \frac{336C^2 + \frac{a_1\varphi_{10}(r)}{a_2^{2/3}a_3^4\chi(r)^{5/3}}}{56C\kappa\left(Cr^2+1\right)^3}, \tag{69}$$

where $\varphi_8(r)$, $\varphi_9(r)$ and $\varphi_{10}(r)$ are auxiliary functions defined in Sect. 13.

So using the matching conditions, we obtain

$$a_1 = \frac{112a_2^{2/3}a_3^4C^2R^2\left(CR^2\left(CR^2+3\right)-6\right)\chi(R)^{2/3}}{3\left(9CR^2+1\right)} \times \Bigg[81a_2^{11/3}C^3 + 14a_3^3\chi(R)^{2/3} - 126a_2a_3^2C\chi(R)^{2/3} + 189a_2^2a_3C^2\chi(R)^{2/3} - 81a_2^3C^3\chi(R)^{2/3} + 27a_2^{8/3}a_3C^2\left(2CR^2-7\right) - 9a_2^{5/3}a_3^2C\left(CR^2\left(CR^2+14\right)-14\right) + a_2^{2/3}a_3^3\left(CR^2\left(CR^2\left(4CR^2+21\right)+84\right)-14\right)\Bigg]^{-1}, \tag{70}$$

$$C = \frac{M}{R^2(4R-9M)}, \tag{71}$$

$$A = \frac{1-\frac{2M}{R}}{\left(\frac{M}{4R-9M}+1\right)^4}. \tag{72}$$

Note that from Eqs.(71) and (72), the solution must satisfy $M/R < 4/9$, which corresponds to the Buchdahl's limit.

11. Results and discussion

In this section, we analyse the physical acceptance of the new models developed in this manuscript, as we will also discuss these results. For such purposes, we had taken into account the compactness factor of the system 4U 1820-30 (see Table 1). Also, we checked that the models behaved regularly if we set the constants a_2 and a_3 in the way of Table 2. It is worth mentioning that these models can be used for other systems by changing the values of the parameters a_2 and a_3 in a correct manner in order to ensure compliance with the physical acceptance conditions.

Table 1. Physical parameters for the compact star 4U 1820-30.

Compact start	$M/M_\odot$	$R(km)$	$u = M/R$	$\rho(0)/\rho(R)$	$Z(R)$
4U 1820-30 [137]	1.58	9.1	0.2501	2.0266 [137]	0.414496

Table 2. Energy density ratio predicted by all new models.

Model	$\rho(0)/\rho(R)$
like-Wyman	2.1263
like-Tolman IV	4.37376
like-Heinztmann	2.16077
like-Durgapal IV	2.15727

11.1. Metrics

The metrics e^{ν} and $e^{-\lambda}$ are plotted in Figs. 1 and 2, respectively. We observe from these figures that condition C1 of Sect. 4 is satisfied for all models. It is interesting that the value of e^{ν} is higher for the Model 1 compared with the other models.

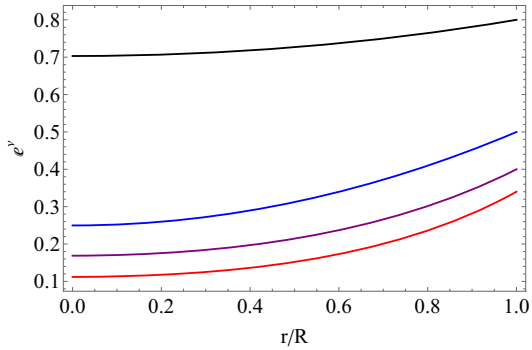

Figure 1. e^{ν} for $u = 0.2501$, Model 1 (black line), Model 2 (blue line), Model 3 (purple line), Model 4 (red line) and parameters in Table 2.

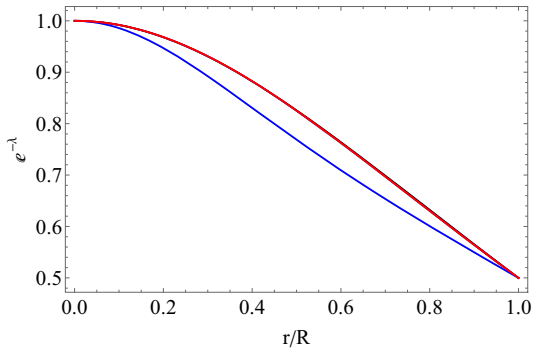

Figure 2. $e^{-\lambda}$ for $u = 0.2501$, Model 1 (black line), Model 2 (blue line), Model 3 (purple line), Model 4 (red line) and parameters in Table 2.

11.2. Matter sector

In Figs. 3, 4 and 5 the energy density, radial and tangential pressures are shown. We can see from these figures that condition C2 is met for all models, namely that the matter sector is positive and regular within the compact object. The energy density, radial pressure, and tangential pressure are decreasing functions of radial coordinate r, having their maximum values at the center of the stellar object. Furthermore, the radial pressure should vanish at the boundary and $p_r|_{r=0} - p_t|_{r=0} = 0$ (See. Fig. 6). At this point, it is worth noting that the behavior of the energy density and the anisotropy pressure for the Model 2 (like-Tolman IV) is distinct from others models.

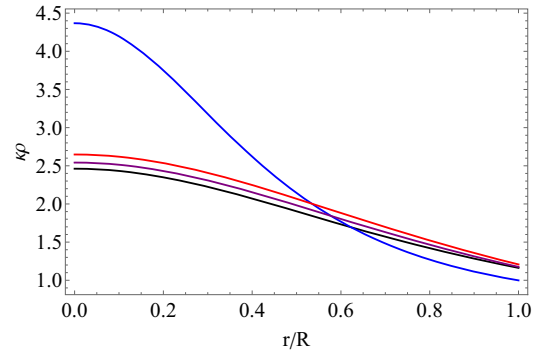

Figure 3. ρ for $u = 0.2501$, Model 1 (black line), Model 2 (blue line), Model 3 (purple line), Model 4 (red line) and parameters in Table 2.

11.3. Dominant Energy conditions and causality

The profiles of $\rho - p_r$ and $\rho - p_t$ are shown in Figs. 7 and 8, respectively. In these figures, we can observe that the DEC is fulfilled by all models. Also, we observe that for the Model 2 the values of these profiles are higher than the rest of the models.

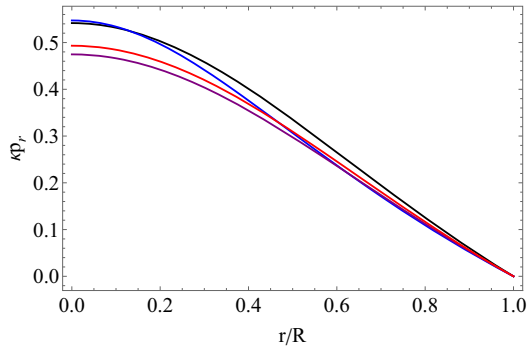

Figure 4. p_r for $u = 0.2501$, Model 1 (black line), Model 2 (blue line), Model 3 (purple line), Model 4 (red line) and parameters in Table 2.

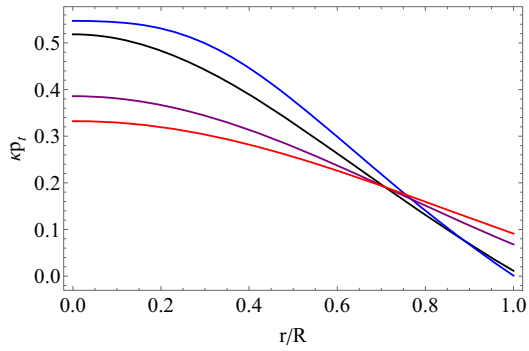

Figure 5. p_t for $u = 0.2501$, Model 1 (black line), Model 2 (blue line), Model 3 (purple line), Model 4 (red line) and parameters in Table 2.

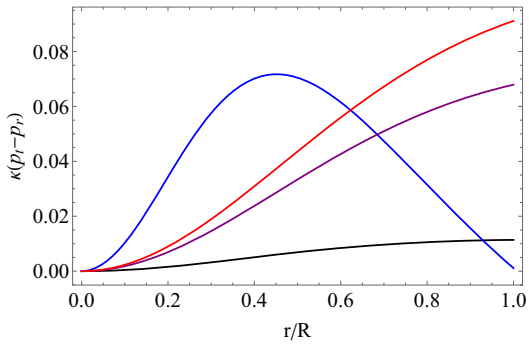

Figure 6. $p_t - p_r$ for $u = 0.2501$, Model 1 (black line), Model 2 (blue line), Model 3 (purple line), Model 4 (red line) and parameters in Table 2.

On the other hand, we plotted the internal sound velocities in the radial and tangential directions in Figs. 9 and 10. We observed from them that condition C5 is satisfied by every model, namely, that they do not surpass the relativistic limit of light velocity. Also, we have to note that for the Model 2 such profiles of sound velocities

have a steeper slope than the rest of the models.

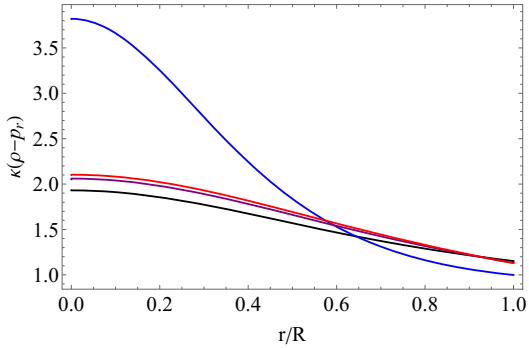

Figure 7. $\rho - p_r$ for $u = 0.2501$, Model 1 (black line), Model 2 (blue line), Model 3 (purple line), Model 4 (red line) and parameters in Table 2.

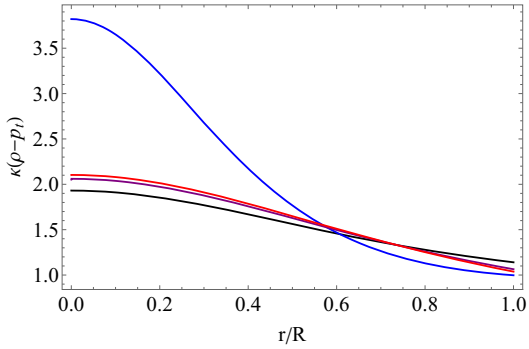

Figure 8. $\rho - p_t$ for $u = 0.2501$, Model 1 (black line), Model 2 (blue line), Model 3 (purple line), Model 4 (red line) and parameters in Table 2.

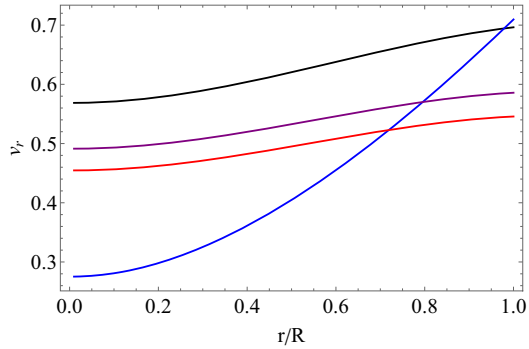

Figure 9. v_r for $u = 0.2501$, Model 1 (black line), Model 2 (blue line), Model 3 (purple line), Model 4 (red line) and parameters in Table 2.

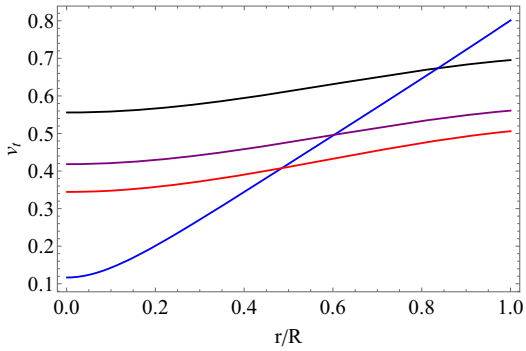

Figure 10. v_t for $u = 0.2501$, Model 1 (black line), Model 2 (blue line), Model 3 (purple line), Model 4 (red line) and parameters in Table 2.

11.4. Redshift

In Fig. 11, the redshift z is plotted. In this figure, we observe that z is a monotonously function of the radial coordinate, having its maximum value at the center of the compact object. Also, it is noticeable that the surface redshift value is below the universal bound of $z_{bound} = 5.211$.

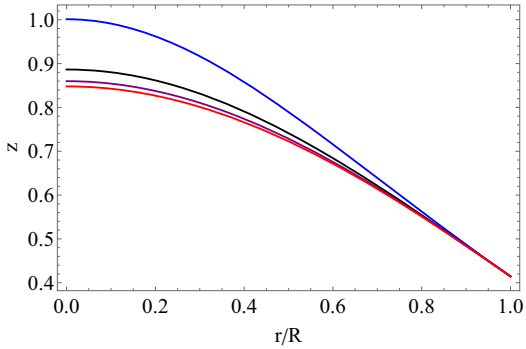

Figure 11. z for $u = 0.2501$, Model 1 (black line), Model 2 (blue line), Model 3 (purple line), Model 4 (red line) and parameters in Table 2.

Because the Model 2 exhibits non-monotonic anisotropy and its sound velocities inside the star exhibit distinct behavior in comparison to the other models, it can be inferred that this model may be unstable. Therefore, in this work, we go one step further and study the stability of the solution in the next two subsections.

11.5. Stability against convection

Any fluid element pushed downward must float back to its original position. Such a principle should be satisfied by any fluid that supports a self-gravitating sphere in order

to remain stable during convection. It was demonstrated in [138] in such a way that

$$\rho'' \leq 0. \tag{73}$$

So in the Fig. 12, the profile of ρ'' is shown. In this figure, we observe that all models do not fulfill this stability condition. Specifically, $\rho'' \leq 0$ is satisfied in the inner regions of the star, while the outer regions are unstable. Furthermore, it is observable that ρ'' has a different behaviour for Model 2 against the other models.

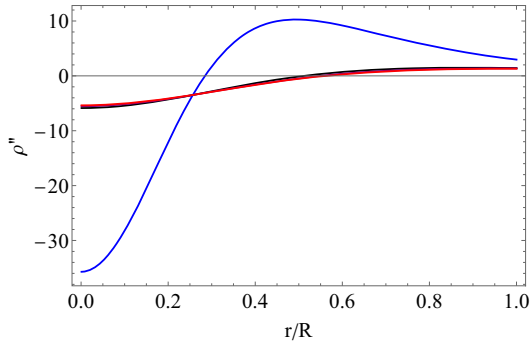

Figure 12. ρ'' for $u = 0.2501$, Model 1 (black line), Model 2 (blue line), Model 3 (purple line), Model 4 (red line) and parameters in Table 2.

11.6. Stability against collapse

In order to study the instability of the models against collapse, it is necessary to analyse the behavior of the adiabatic index (Γ) in the radial direction given by

$$\Gamma = \frac{\rho + p_r}{p_r}\frac{dp_r}{d\rho}, \tag{74}$$

which should satisfy

$$\Gamma \geq \Gamma_{crit}, \tag{75}$$

with

$$\Gamma_{crit} = \frac{4}{3} + \frac{19}{21}\frac{M}{R}. \tag{76}$$

The relationship mentioned above accounts for relativistic adjustments to the adiabatic index Γ that can cause instabilities inside the star. So in this way, the stability condition (76) applies to any relativistic compact object supported by an anisotropic fluid (for a detailed discussion about this point, see Refs. [73, 139, 140].

The adiabatic index profile is then displayed in Fig. 13 as a function of radial coordinate. It is observable from this figure that the Model 2 presents instability against collapse for the parameters shown in the caption. While, in the rest of the models, we checked that they have stability against collapse, namely, that they satisfy the condition (75).

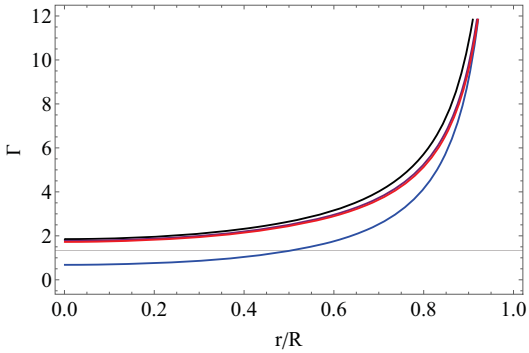

Figure 13. Γ for $u = 0.2501$, Model 1 (black line), Model 2 (blue line), Model 3 (purple line), Model 4 (red line) and parameters in Table 2.

Now, the density ratio for the system 4U 1820-30 is $\rho(0)/\rho(R) \approx 2.0266$ [137], which is near the predictions of Model 1, Model 3 and Model 4 (see Table 2). While the value predicted by Model 2 is so far with this value. Then, we have that the Model 1, Model 2 and Model 3 are appropriate in order to model the system 4U 1820-30, and the Model 2 results inadequate in such purpose.

12. Final Remarks

In conclusion, the models constructed in this work satisfy the essential physical requirements listed in Sect. 4, namely, they have the regular behavior of a realistic stellar compact object for the parameters shown in Table 2. Respecting the relation of energy density $\rho(0)/\rho(R)$ results in all models fitting accurately to the system 4U 1820-30 except for the Model 2 which departures from the value of such ratio. Instability against convective motion is nonetheless presented by the models. But on the other hand, all of the other models, with the exception of Model 2, exhibit stability in the face of collapse. Therefore, it may be worth conducting a study in the future of the behavior of the matter sector of these models against small perturbations and being able to relate the results to those found here in Sect. 11.5 and 11.6. Moreover, the current work is important given that, together with the previous works [90,91], they are evidence that GD can be used through the MGD together with a non-zero complexity factor condition in order to find new families of anisotropic interior solutions, which can also be regulated through their parameters to be able to model some realistic compact stellar systems.

Finally, it would be very interesting to use the same technique performed here in order to find new anisotropic solutions with other generalizations of the complexity factor of a known solution or to use the extended version of the MGD instead of the MGD. It is worth noting that not only new solutions with vanishing complexity are valuable, but also solutions with non vanishing complexity should be interesting. Of course, this would imply a complicated mathematical challenge when it comes to

considering geometric deformation in both metrics, radial and temporal, which, to date, with the exception of the use of vanishing complexity, has not been done already.

13. Appendix: Auxiliary functions

$$
\begin{aligned}
\chi &= a_2 + a_3 r^2 \\
\varphi_1 &= a_3 r^2 (15 a_2 B_0 - A_0 a_3) + 3 a_2 (a_3 A_0 + 3 a_2 B_0) + 10 a_3^2 B_0 r^4 \\
\varphi_2 &= a_3 A_0 + 3 a_2 B_0 + 2 a_3 B_0 r^2 \\
\varphi_3 &= 2 a_2 a_3 A_0 + a_3^2 A_0 r^2 + 6 a_2^2 B_0 - 6 \sqrt[3]{a_2} B_0 \chi(r)^{5/3} \\
&\quad + 10 a_2 a_3 B_0 r^2 + 5 a_3^2 B_0 r^4 \\
\varphi_4 &= 27 a_2^{11/3} B^2 \left(B r^2 - 1\right) \\
&\quad - 27 a_2^3 B^2 \left(B r^2 - 1\right) \chi(r)^{2/3} \\
&\quad - 6 a_3^3 r^2 \left(B r^2 - 1\right) \chi(r)^{2/3} \\
&\quad + 3 a_2^{5/3} a_3^2 \left(B r^2 - 1\right) \left(5 B r^2 \left(B r^2 - 4\right) + 2\right) \\
&\quad + 9 a_2^{8/3} a_3 B \left(B r^2 \left(5 B r^2 - 9\right) + 4\right) \\
&\quad - 9 a_2^2 a_3 B \left(B r^2 \left(3 B r^2 - 7\right) + 4\right) \chi(r)^{2/3} \\
&\quad + 6 a_2 a_3^2 \left(B r^2 \left(6 B r^2 - 7\right) + 1\right) \chi(r)^{2/3} \\
&\quad + a_2^{2/3} a_3^3 r^2 \left(B r^2 \left(B r^2 \left(5 B r^2 + 3\right) + 54\right) + 2\right) \\
\varphi_5 &= 9 a_2^2 B^2 + 6 a_2 a_3 B \left(B r^2 - 2\right) - a_3^2 \left(B r^2 \left(B r^2 + 8\right) - 2\right) \\
\varphi_6 &= 135 a_2^{11/3} B^3 - 135 a_2^3 B^3 \chi(r)^{2/3} \\
&\quad - 30 a_3^3 B r^2 \chi(r)^{2/3} \\
&\quad + 45 a_2^2 a_3 B^2 \left(4 - 3 B r^2\right) \chi(r)^{2/3} \\
&\quad + 45 a_2^{8/3} a_3 B^2 \left(5 B r^2 - 4\right) \\
&\quad + 30 a_2 a_3^2 B \left(6 B r^2 - 1\right) \chi(r)^{2/3} \\
&\quad + 15 a_2^{5/3} a_3^2 B \left(5 B r^2 \left(B r^2 - 4\right) + 2\right) \\
&\quad - a_2^{2/3} a_3^3 \left(B r^2 \left(B r^2 \left(31 B r^2 + 156\right) - 6\right) + 4\right) \\
\varphi_7 &= -81 a_2^3 C^3 + 27 a_2^2 a_3 C^2 \left(7 - 2 c r^2\right) \\
&\quad + 9 a_2 a_3^2 C \left(C r^2 \left(C r^2 + 14\right) - 14\right) \\
&\quad - \left(a_3^3 \left(C r^2 \left(C r^2 \left(4 C r^2 + 21\right) + 84\right) - 14\right)\right) \\
\varphi_8 &= 243 a_2^{14/3} C^3 \left(1 - 3 C r^2\right) \\
&\quad + 42 a_3^4 r^2 \left(1 - 3 C r^2\right) \chi(r)^{2/3} \\
&\quad + 243 a_2^4 C^3 \left(3 C r^2 - 1\right) \chi(r)^{2/3} \\
&\quad - 81 a_2^{11/3} a_3 C^2 \left(3 C r^2 - 1\right) \left(5 C r^2 - 7\right) \\
&\quad + 42 a_2 a_3^3 \left(3 C r^2 - 1\right) \left(9 C r^2 - 1\right) \chi(r)^{2/3}
\end{aligned}
$$

$$
\begin{aligned}
&- 27a_2^{8/3}a_3^2C\left(3Cr^2-1\right)\left(5Cr^2\left(Cr^2-7\right)+14\right)\\
&- 189a_2^2a_3^2C\left(9Cr^2\left(Cr^2-1\right)+2\right)\chi(r)^{2/3}\\
&+ 81a_2^3a_3C^2\left(3Cr^2\left(3Cr^2-8\right)+7\right)\chi(r)^{2/3}\\
&+ 3a_2^{5/3}a_3^3\left(3Cr^2-1\right)\varphi_{11}+a_2^{2/3}a_3^4r^2\varphi_{12}\\
\varphi_9 \;=\; &- 81a_2^3C^3+27a_2^2a_3C^2\left(7-2Cr^2\right)\\
&+ 9a_2a_3^2C\left(Cr^2\left(Cr^2+14\right)-14\right)\\
&- \left(a_3^3\left(Cr^2\left(Cr^2\left(4Cr^2+21\right)+84\right)-14\right)\right)\\
\varphi_{10} = \;&- 729a_2^{14/3}C^4+a_2^{2/3}a_3^4\varphi_{13}(r)\\
&+ 729a_2^4C^4\chi(r)^{2/3}-126a_3^4Cr^2\chi(r)^{2/3}\\
&+ 243a_2^3a_3C^3\left(3Cr^2-7\right)\chi(r)^{2/3}\\
&- 567a_2^2a_3^2C^2\left(3Cr^2-2\right)\chi(r)^{2/3}\\
&+ 126a_2a_3^3C\left(9Cr^2-1\right)\chi(r)^{2/3}\\
&- 243a_2^{11/3}a_3C^3\left(5Cr^2-7\right)\\
&- 81a_2^{8/3}a_3^2C^2\left(5Cr^2\left(Cr^2-7\right)+14\right)\\
&+ 9a_2^{5/3}a_3^3C\left(5Cr^2\left(Cr^2\left(Cr^2+21\right)-42\right)+14\right)\\
\varphi_{11} = \;&5Cr^2\left(Cr^2\left(Cr^2+21\right)-42\right)+14\\
\varphi_{12} = \;&Cr^2\left(Cr^2\left(Cr^2\left(20Cr^2+47\right)-357\right)+602\right)+14\\
\varphi_{13} = \;&14+Cr^2\left(Cr^2\left(Cr^2\left(106Cr^2+413\right)+1008\right)-14\right).
\end{aligned}
$$

14. References

[1] K. Schwarzschild, Sitz. Deut. Akad. Wiss. Berlin Kl. Math. Phys. 1, 189 (1916).
[2] M.K. Mak, T. Harko. Eur. Phys. J. C **73**, 2585 (2013) .
[3] M. Sharif, M. Waseem, Eur. Phys. J. Plus **131**, 190 (2016).
[4] S. Kumar, Y. K. Gupta, & J. R. Sharma. Int. J. Eng. Math. Phys. Sci. 3.0(2) (2010).
[5] B. Chilambwe, S. Hansraj, Eur. Phys. J. Plus **130**, 19 (2015).
[6] S. Thirukkanesh and S. D. Maharaj, Class. Quantum Grav. **23** 2697 (2006).
[7] A.K. Prasad, J. Kumar & A. Kumar, Arab. J. Math. **10**, 669–683 (2021).
[8] S. Rahman and M. Visser, Class. Quant. Grav. **19**, 935 (2002).
[9] K. Lake, Phys. Rev. D **67**, 104015 (2003).
[10] D. Martin, & M. Visser, Phys. Rev. D **69**, 104028 (2004).
[11] P. Boonserm, M. Visser, and S. Weinfurtner Phys. Rev. D **71**, 124037 (2005).
[12] S. Hansraj, L. Moodly, Eur. Phys. J. C **80**, 496 (2020).
[13] D. Kileba Matondo, S.D. Maharaj & S. Ray, Astrophys Space Sci **363**, 187 (2018).
[14] J. Kumar, P. Bharti, Pramana - J Phys **96**, 156 (2022).
[15] A. Banerjee and N. O. Santos, J. Math. Phys. **22**, 824 (1981).
[16] P. S. Florides, J. Phys. A: Math. Gen. **16** 1419 (1983).
[17] D. C. Srivastava, Fortschritte der Physik/Progress of Physics, **40**(1), 31 (1992).
[18] S.N. Pandey and R. Tiwari, Indian Journal of Pure and Applied Mathematics, **12**(2), 261 (1981).
[19] R.C. Tolman, Phys. Rev. **55**(4), 364 (1939).
[20] M.S.R. Delgaty, K. Lake, Comput. Phys. Commun. **115**(2–3), 395 (1998).

[21] J. Estevez-Delgado, Cabrera, J. V. Paulin-Fuentes, J. M. Rodriguez Ceballos, J. A. & M. P. Duran, Modern Physics Letters A, **35**(15), 2050120 (2020).
[22] G. Estevez-Delgado, J. Estevez-Delgado, M. Pineda Duran, N. Montelongo García, & J. M. Paulin-Fuentes, Revista mexicana de física, **65**(4), 382 (2019).
[23] G. Estevez-Delgado, J. Estevez-Delgado, N. M. García, & M. P. Duran, Canadian Journal of Physics, **97**(9), 988 (2019).
[24] G. Estevez-Delgado, et al., Modern Physics Letters A **34**.15, 1950115 (2019).
[25] M. F. Shamir, G. Mustafa, & Q. Hanif, International Journal of Modern Physics A, **35**(18), 2050083 (2020).
[26] D. Ida, Progress of theoretical physics **103**.3, 573 (2000).
[27] N. Pant, & S. Faruqi, Gravitation and Cosmology, **18**(3), 204 (2012).
[28] M. H. Murad, & S. Fatema, Astrophysics and space science, **343**(2), 587 (2013).
[29] C. G. Boehmer, & A. Mussa, General Relativity and Gravitation, **43**(11), 3033 (2011).
[30] S. S. Yazadjiev, Modern Physics Letters A, **20**(11), 821 (2005).
[31] Errehymy, Abdelghani, et al., New Astronomy, 101957 (2022).
[32] J. Andrade, D. Santana. Eur. Phys. J. C **82**, 985 (2022).
[33] L. Herrera, N.O. Santos, Phys. Rep. **286**, 53 (1997).
[34] M. Ruderman, Annual Review of Astronomy and Astrophysics, **10**, 427 (1972).
[35] R. Kippenhahn, A. Weigert , Stellar Structure and Evolution, 2nd edn. (Springer, New York, 1990).
[36] A.I. Sokolov, Sov. Phys. JETP 52(4), 575 (1980).
[37] R.F. Sawyer, Phys. Rev. Lett. 29(6), 382 (1972).
[38] J. B. Hartle, R. Sawyer, and D. Scalapino, Astrophys. J. **199**, 471 (1975).
[39] S. Bayin, Phys. Rev. D **26**, 1262 (1982).
[40] D. Reimers, S. Jordan, D. Koester, N. Bade, T. Kohler, L. Wisotzki, Astron. Astrophys. **311**, 572 (1996).
[41] A.P. Martinez, R.G. Felipe, D.M. Paret, Int. J. Mod. Phys. D **19**, 1511 (2010).
[42] R. Chan, L. Herrera, N.O. Santos, Mon. Not. R. Astron. Soc. **265**, 533 (1993).
[43] L. Herrera, A. Di Prisco, J. Martin, J. Ospino, N.O. Santos, O. Troconis, Phys. Rev. D **69**, 084026 (2004).
[44] E.N. Glass, Gen. Relativ. Gravit. **45**, 2661 (2013).
[45] L. Herrera, J. Ospino, A. Di Prisco, Phys. Rev. D **77**, 027502 (2008).
[46] P.H. Nguyen, J.F. Pedraza, Phys. Rev. D **88**, 064020 (2013).
[47] J. Krisch, E.N. Glass, J. Math. Phys. **54**, 082501 (2013).
[48] R. Sharma, B. Ratanpal, Int. J. Mod. Phys. D **22**, 1350074 (2013).
[49] K.P. Reddy, M. Govender, S.D. Maharaj, Gen. Relativ. Gravit. **47**, 35 (2015).
[50] M. Esculpi, M. Malaver, & E. A. Aloma, Gen Relativ Gravit **39**, 633 (2007).
[51] V. Folomeev and V. Dzhunushaliev, Phys. Rev. D **91**, 044040 (2015).
[52] A. A. Isayev, and J. Yang. Phys. Lett. B **707**.1, 163 (2012).
[53] L. Herrera, Phys. Rev.D **101**, 104024 (2020).
[54] M.K. Mak, T. Harko, Proc. R. Soc. Lond. A **459**, 393 (2003).
[55] S.K. Maurya, S.D. Maharaj, Eur. Phys. J. C 77, 328 (2017).
[56] Ovalle, Mod. Phys. Lett. A 23, 3247 (2008).
[57] J. Ovalle, "Braneworld stars: anisotropy minimally projected onto the brane" Gravitation and Astrophysics. 173-182 (2010).
[58] J. Ovalle, Phys. Rev. D **95**, 104019 (2017).
[59] J. Ovalle, R. Casadio, R. da Rocha, A. Sotomayor, Eur. Phys. J. C **78**, 122 (2018).
[60] J. Ovalle, and R. Casadio. Beyond Einstein Gravity: The Minimal Geometric Deformation Approach in the Brane-World. Springer Nature, 2020.
[61] J. Ovalle, Phys. Lett. B 788, 213 (2019).J. Ovalle, Phys. Lett. B **788**, 213 (2019).
[62] K.N. Singh, S.K. Maurya, M.K. Jasim, et al. Eur. Phys. J. C **79**, 851 (2019).

[63] L. Gabbanelli, A. Rincón, C. Rubio, Eur. Phys. J. C **78**(5), 370 (2018).
[64] R.P. Graterol, Eur. Phys. J. Plus **133**, 244 (2018).
[65] E. Morales, F. Tello-Ortiz, Eur. Phys. J. C **78**, 841 (2018).
[66] F. Tello-Ortiz. Eur. Phys. J. C **80**, 413 (2020).
[67] F. Tello-Ortiz et al., Chinese Phys. C **44** 105102 (2020).
[68] S.K. Maurya, F. Tello-Ortiz, Eur. Phys. J. C **79**, 85 (2019).
[69] V.A. Torres, E.Contreras, Eur. Phys. J.C **79**(10), 1 (2019).
[70] S. Hensh, Z. Stuchlík, Eur. Phys. J. C **79**, 834 (2019).
[71] G. Abellán, Á. Rincón, E. Fuenmayor et al., Eur. Phys. J. Plus **135**, 606 (2020).
[72] C. Las Heras, P. León, Eur. Phys. J. C **79**, 990 (2019).
[73] F. Tello-Ortiz, S.K. Maurya, Y. Gomez-Leyton, Phys. J. C **80**, 324 (2020).
[74] P. Tamta and P. Fuloria. Phys. Scr. **96** 095003 (2021).
[75] S.K. Maurya, K.N. Singh, & B. Dayanandan, Eur. Phys. J. C **80**, 448 (2020).
[76] S.K. Maurya, Eur. Phys. J. C **79**, 958 (2019).
[77] B. Dayanandan et al. Phys. Scr. **96** 125041 (2021).
[78] D. Santana, E. Fuenmayor & E. Contreras, Eur. Phys. J. C **82**, 703 (2022).
[79] S. K. Maurya et al., Physica Scripta **97**.10 105002 (2022).
[80] M. Zubair, and H. Azmat, Annals of Physics **420** 168248 (2020).
[81] M. Zubair, Mobeen Amin, and Hina Azmat. Physica Scripta 96.12: 125008 (2021).
[82] E. Morales, F. Tello-Ortiz, Eur. Phys. J. C **78**, 618 (2018).
[83] Y. Gomez-Leyton, et al. Physica Scripta 96.2: 025001 (2020).
[84] S. K. Maurya, F. Tello-Ortiz. Eur. Phys. J. C **79**, 33 (2019).
[85] C. Arias, F. Tello-Ortiz & E. Contreras. Eur. Phys. J. C 80, 463 (2020).
[86] M. Sharif, S. Sadiq. Eur. Phys. J. C **78**, 410 (2018).
[87] J Ovalle et al. Class. Quantum Grav. **36** 205010 (2019).
[88] L. Herrera, Phys. Rev. D **97**, 044010 (2018).
[89] L. Herrera, Entropy **23**, 802 4 of 5 (2021).
[90] J. Andrade, Contreras, E. Stellar models with like-Tolman IV complexity factor. Eur. Phys. J. C **81**, 889 (2021).
[91] J. Andrade, E. Fuenmayor, and E. Contreras, International Journal of Modern Physics D **31**.12 2250093 (2022).
[92] S. K. Maurya, A. Errehymy, R. Nag, and M. Daoud, Fortschr. Phys **70**, 2200041 (2022).
[93] M. Carrasco-Hidalgo, E. Contreras, Eur. Phys. J. C **81**, 757 (2021).
[94] Casadio, R., Contreras, E., Ovalle, J. et al. Eur. Phys. J. C **79**, 826 (2019).
[95] E. Contreras, E. Fuenmayor & G. Abellán, Eur. Phys. J. C **82**, 187 (2022).
[96] C. Arias, E. Contreras, E. Fuenmayor, A. Ramos, Annals of Physics, **436**, 168671 (2022).
[97] S.K. Maurya, M. Govender, S. Kaur et al. Eur. Phys. J. C **82**, 100 (2022).
[98] M. Sharif, A. Majid, Eur. Phys. J. Plus **137**, 114 (2022).
[99] J. Andrade, Eur. Phys. J. C **82**, 266 (2022).
[100] J. Andrade, The European Physical Journal C, **82**(7), 1 (2022).
[101] E. Contreras, Z. Stuchlik, Eur. Phys. J. C **82**, 706 (2022).
[102] S. Sadiq, and R. Saleem, Chinese Journal of Physics **79** 348 (2022).
[103] M. Zubair, Eur. Phys. J. C **82**, 984 (2022).
[104] P. Bargueño, E. Fuenmayor, and E. Contreras, Annals of Physics **443** 169012 (2022).
[105] R. Avalos, E. Fuenmayor, & E. Contreras, Eur. Phys. J. C **82**, 420 (2022).
[106] R. Avalos, and E. Contreras. "Quasi Normal Modes of a Like–Casimir Traversable Wormhole Through the 13thorder."
[107] M. Govender, W. Govender, G. Govender et al., Eur. Phys. J. C **82**, 832 (2022).
[108] L. Herrera, A. Di Prisco, J. Ospino, Phys. Rev. D **98**, 104059 (2018).
[109] R.S. Bogadi, M. Govender, Eur. Phys. J. C **82**, 475 (2022).
[110] L. Herrera, A.D. Prisco, J. Ospino, Phys. Rev. D **99**, 044049 (2019).

[111] U Farwa et al. Phys. Scr. 97 105307 (2022).
[112] M. Sharif, I.I. Butt. Eur. Phys. J. C **78**, 850 (2018).
[113] S. Khan, S.A. Mardan & M.A. Rehman. Eur. Phys. J. C **81**, 831 (2021).
[114] M. Sharif, and T. Naseer. "Complexity of dynamical dissipative cylindrical system in non-minimally coupled theory." Chinese Journal of Physics (2022).
[115] L. Herrera, A. Di Prisco, and J. Ospino. Phys. Rev. D **103**, 024037 (2021).
[116] L. Herrera L, A. Di Prisco, J. Ospino. Symmetry. 2021; **13**(9):1568.
[117] L. Herrera, A. Di Prisco, and J. Ospino. Entropy **23**.9: 1219 (2021).
[118] Herrera, L. "Non-static hyperbolicallly symmetric fluids." arXiv preprint arXiv:2208.10986 (2022).
[119] Z. Yousaf, M.Z. Bhatti, M. Khlopov, H. Asad, Entropy **24**, 150 (2022).
[120] Z. Yousaf, et al. Universe **8**.6: 337 (2022).
[121] Z. Yousaf, et al. "Hyperbolically symmetric static charged cosmological fluid models." Monthly Notices of the Royal Astronomical Society **510**.3: 4100-4109 (2022).
[122] Z. Yousaf et al. Phys. Scr. 97 055304 (2022).
[123] M. Z. Bhatti, Z. Yousaf & S. Hanif. Eur. Phys. J. Plus **137**, 65 (2022).
[124] Z. Yousaf. Universe **8**.2: 131 (2022).
[125] M.Z. Bhatti, Z. Yousaf & Z. Tariq. Eur. Phys. J. Plus **136**, 857 (2021).
[126] Z. Yousaf, M. Z. Bhatti, and H. Asad. Annals of Physics **437**: 168753 (2022).
[127] M. Z. Bhatti, Z. Yousaf & Z. Tariq. Eur. Phys. J. C **81**, 1070 (2021).
[128] M. Z. Bhatti, Z. Yousaf & S. Hanif. Eur. Phys. J. C **82**, 340 (2022).
[129] B.V. Ivanov, Eur. Phys. J. C **77**, 738 (2017).
[130] B.V. Ivanov, Phys. Rev. D **65**(10), 104011 (2002).
[131] L. Bel, Ann. Inst. Henri Poincaré **17**, 37 (1961).
[132] A.G.P. Gómez-Lobo, Class. Quantum Gravity **25**,015006 (2007).
[133] L. Herrera, J. Ospino, A. Di Prisco, E. Fuenmayor, O. Troconis, Phys. Rev. D **79**, 064025–12 (2009).
[134] M. Wyman, Phys. Rev. **75**(12), 1930 (1949).
[135] H. Heintzmann, Z. Phys. **228**(4), 489 (1969).
[136] M.C. Durgapal, J. Phys. A Math. Gen. **15**(8), 2637 (1982).
[137] A.K. Prasad, J. Kumar, S.K. Maurya et al., Astrophys Space Sci **364**, 66 (2019).
[138] H. Hernández, L. Núñez, A. Vázques, Eur. Phys. J. C **78**, 883 (2018).
[139] C.C. Moustakidis, Gen. Relativ. Gravit. **49**, 68 (2017).
[140] S.K. Maurya, R. Nag, Eur. Phys. J. Plus **136**, 679 (2021).